4720 J. Med. Chem. 2010, 53, 4720–4730
DOI: 10.1021/jm100230k

Journal of Medicinal Chemistry Article

Online Fluorescence Enhancement Assay for the Acetylcholine Binding Protein with Parallel Mass Spectrometric Identification

Jeroen Kool,*[,†,∥] Gerdien E. de Kloe,[‡,∥] Ben Bruyneel,[†] Jon S. de Vlieger,[†] Kim Retra,[†] Maikel Wijtmans,[‡] Rene van Elk,[§] August B. Smit,[§] Rob Leurs,[‡] Henk Lingeman,[†] Iwan J.P. de Esch,[‡] and Hubertus Irth[†]

[†]*BioMolecular Analysis, Department of Chemistry and Pharmaceutical Sciences, Faculty of Sciences, VU University Amsterdam, De Boelelaan 1083, 1081HV Amsterdam, The Netherlands,* [‡]*Medicinal Chemistry, Department of Chemistry and Pharmaceutical Sciences, Faculty of Sciences, VU University Amsterdam, The Netherlands, and* [§]*Molecular and Cellular Neurobiology, Center for Neurogenomics and Cognitive Research, Neuroscience Campus Amsterdam, VU University Amsterdam, The Netherlands.* [∥]*Both authors contributed equally to this work.*

Received February 22, 2010

The acetylcholine binding protein (AChBP) is considered an analogue for the ligand-binding domain of neuronal nicotinic acetylcholine receptors (nAChRs). Its stability and solubility in aqueous buffer allowed the development of an online bioaffinity analysis system. For this, a tracer ligand which displays enhanced fluorescence in the binding pocket of AChBP was identified from a concise series of synthetic benzylidene anabaseines. Evaluation and optimization of the bioaffinity assay was performed in a convenient microplate reader format and subsequently transferred to the online format. The high reproducibility has the prospect of estimating the affinities of ligands from an in-house drug discovery library injected in one known concentration. Furthermore, the online bioaffinity analysis system could also be applied to mixture analysis by using gradient HPLC. This led to the possibility of affinity ranking of ligands in mixtures with parallel high-resolution mass spectrometry for compound identification.

Introduction

The nicotinic acetylcholine receptor (nAChR[a]) family is considered one of the most intensively studied ligand-gated ion channels and constitutes valid pharmaceutical targets for pain relief, Alzheimer's disease, Parkinson's disease, epilepsy, anxiety, and several cognitive and attention deficits.[1−5] Analysis of ligand binding to nAChRs is usually conducted by low-throughput electrophysiological patch-clamping methodologies or radioligand binding analysis. Although patch-clamping is automated today, this is still a cumbersome and time-consuming endeavor. Radioligand binding assays (RBAs), on the other hand, suffer from problems associated with the use of radioactive materials and heterogeneous assay formats. For screening purposes, assays based on frontal affinity chromatography have been developed.[6−8] These methodologies, however, suffer from relatively long analysis times.

The acetylcholine binding protein (AChBP) is a structural analogue of the extracellular ligand binding domain of nAChRs. It displays comparable ligand pharmacology to the α7 nAChR in particular.[1,5] AChBPs originate from mollusks, and since the first crystal structure was published in 2001,[9] it has become a model to identify novel ligands for nAChRs by design-intensive methods. The stable and water-soluble protein, which can be produced in large quantities, opened new opportunities for biochemical assays. Methods like SPR and NMR[10] can be used for screening and also, together with tryptophan fluorescence,[11] for gaining insights into AChBP functioning. All these technologies, however, are hampered by background interferences, low sensitivities and/or long analysis times. Furthermore, they are most suitable for analyzing pure compounds.

We now present an online bioaffinity analysis methodology for AChBP based on fluorescence-enhancement with parallel mass spectrometric detection. Online bioaffinity analysis is based on continuous flow assays[12,13] and could be perfectly used for screening compound libraries when based on fluorescence enhancement of a tracer ligand and performed in flow injection mode. These assay formats, including the current one, are usually easily automated, robust, and sensitive. Furthermore, online bioaffinity analysis is ideally suited for mixture analysis when performed in postcolumn format, coupled in parallel to mass spectrometry (MS) to directly link affinities to the corresponding mass spectra.[14]

For development of the online bioaffinity analysis system, a small set of ligands with anticipated fluorescence enhancement properties in the AChBP's binding pocket was synthesized and analyzed. A disubstituted benzylidene anabaseine ligand was chosen as the most efficient tracer. Subsequent focus was on obtaining a very high reproducibility of the final system in order to allow affinity estimation of ligands from our in-house compound library when injected at only one concentration. Finally, the system was used in gradient HPLC mode to rank affinities of ligands in a mixture with a single concentration analysis.

*To whom correspondence should be addressed. Phone: 0031-205987542. Fax: 0031-205987543. E-mail: j.kool@few.vu.nl.

[a]Abbreviations: AChBP, acetylcholine binding protein; Ls, *Lymnaea stagnalis*; nAChR, nicotinic acetylcholine receptor; SPR, surface plasmon resonance; NMR, nuclear magnetic resonance; HPLC, high performance liquid chromatography; HR-MS, high resolution mass spectrometry; RBA, radioligand binding assay.

 Published on Web 06/02/2010

Scheme 1. Synthetic Route to Benzylidene Anabaseines (**6**−**17**) and of Precursors **19**−**20**[a]

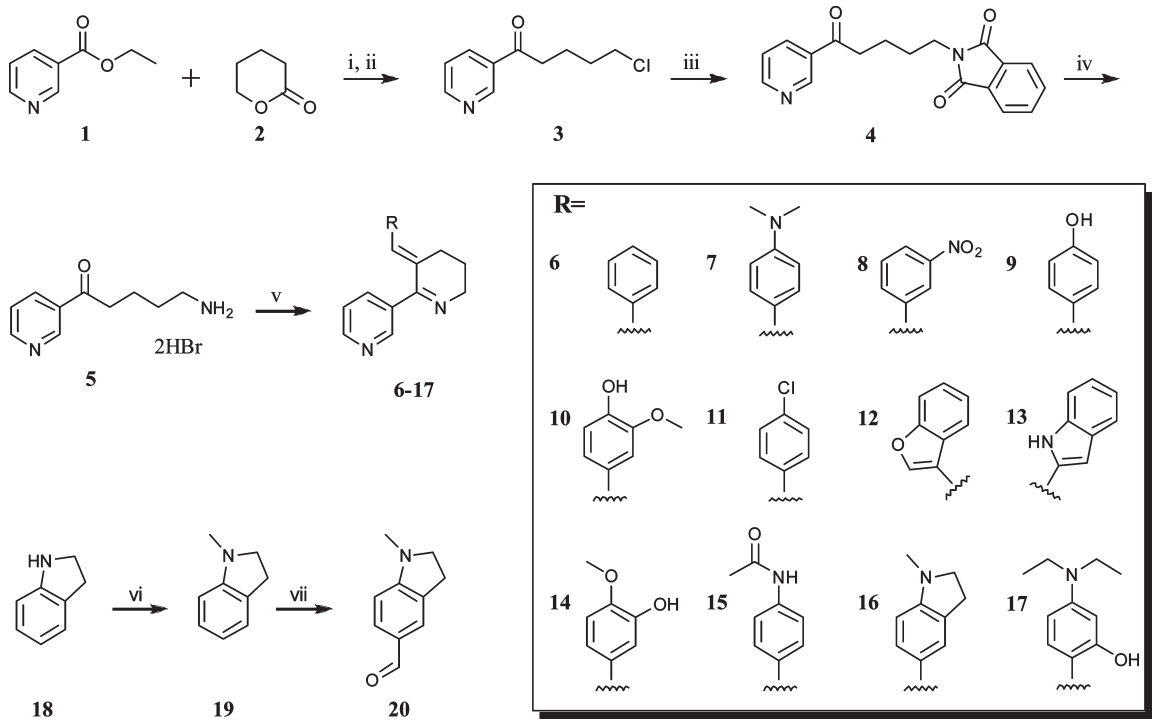

[a] (i) NaH, THF, 0°C−rt; (ii) conc aq HCl, reflux; (iii) potassium phthalimide, K_2CO_3, NMP, 90°C; (iv) conc aq HBr, reflux; (v) substituted benzaldehyde, acetic acid, sodium acetate, methanol, reflux; (vi) Me_2CO_3, K_2CO_3, DMF, reflux; (vii) DMF, $POCl_3$, 1,2-DCE, reflux.

Results and Discussion

Development of a Suitable Tracer Ligand. For the design of our fluorescence enhancement ligand, we turned to benzylidene anabaseine as a core structure based on previously demonstrated fluorescence enhancement of 4-dimethylaminobenzylidene anabaseine (**7**; see Scheme 1) in the active site of AChBP.[15] Fluorescence enhancement in the bound state is thought to be a result of reduced rotational freedom of the ligand due to its binding in the active site.[15] A concise structure−activity relationship (SAR) study around the anabaseine scaffold was initiated. Starting from ethylnicotinate (**1**) and δ-valerolactone (**2**), chloro-precursor **3** was synthesized and substituted by an amine via introduction and deprotection of a phthalimide to give the open (salt) form of anabaseine (**5**). This anabaseine salt could be reacted with several commercially available substituted (benz)aldehydes. Only 1-methylindoline-5-carbaldehyde (**20**) was not available, and therefore synthesized from indoline (**18**) by methylation and Vilsmeier−Haack introduction of the aldehyde. Various substituents at the benzylidene moiety were explored, and an overview of the spectral properties of all benzylidene anabaseines is given in the Supporting Information, Table S-1. A large distribution of λ_{max} values is obtained, representing the differences in electronic properties of the substituents on the benzylidene moiety (**8**−**15**). For compounds with λ_{max} values below 400 nm, no fluorescence enhancement was measured because higher excitation wavelengths are preferred to diminish protein fluorescence background and avoid protein destruction. For compounds with λ_{max} values above 400 nm, fluorescence enhancement in the presence of AChBP was measured (see Table 1). The only two compounds of the initial series with λ_{max} values higher than 400 nm, the 3-methoxy-4-hydroxybenzylidene anabaseine **10** and indole-containing anabaseine **13**, showed minor fluorescence enhancement in the active site of AChBP. Two strategies included in the SAR had the aim of improving the push−pull character of **7**. Incorporation of the aniline moiety in a ring should improve its electron-donating properties by increasing the overlap of the lone pair of the nitrogen with the π-system (**16**), while *N*,*N*-diethylation combined with introduction of an extra electron-donating substituent at the *ortho*-position yielded **17**. Indeed, compounds **16** and **17** both have high λ_{max} values and, especially **17**, display significant fluorescence enhancement upon binding to AChBP (Table 1). On the basis of a balanced evaluation of spectral properties, 4-diethylamino-2-hydroxybenzylidene anabaseine (**17**, DAHBA) emerged as the most suitable displacement ligand for the online bioaffinity analysis system.

Fluorescence Enhancement Assay Development in Microplate Reader Format. The bioaffinity assay was first optimized in microplate reader format; the results obtained were used to determine the assay conditions for the online bioaffinity analysis system. The principle of the assay is based on the competition of ligands with tracer ligand DAHBA that shows fluorescence enhancement in the binding pocket of AChBP. To this end, the high affinity compound epibatidine was used as competing ligand in all evaluation and optimization experiments. For the first evaluation experiment, the concentration of DAHBA was varied (see Figure 1A), while for every concentration of DAHBA, a complete epibatidine IC_{50} curve was constructed. From Figure 1A, it is seen that the assay window increased with higher concentrations of DAHBA until the B_{max} value was reached. At that point, only the background increased as a result of higher concentrations of nonbound DAHBA, but not the assay window. At much higher DAHBA concentrations than its pK_i, also higher concentrations of epibatidine are needed for displacement as seen in Figure 1A by shifting of the IC_{50} curves.

Table 1. Spectral Properties of Benzylidene Anabaseines

no.	λ_{max} (nm)	ε (L mol^{-1} cm^{-1})	fluorescence without AChBP[a]	fluorescence with AChBP[b]	enhancement[c]	$\lambda_{em.}$ (nm)
7	474	42617	1.15	6.15	5.35	537
10	476	17418	0.58	0.58	1	524
13	425	142	4.85	5.15	1.06[d]	493
16	493	21745	0.65	1.60	2.46	543
17	489	65261	3.60	20.80	5.78	533

[a] Measured for 5 μM conc in buffer, pH = 7.4. [b] Measured with a final concentration Ls-AChBP of 42 nM. [c] Defined as fluorescence in presence of Ls-AChBP divided by fluorescence in absence of Ls-AChBP. [d] Measured at 5×10^{-4} M conc.

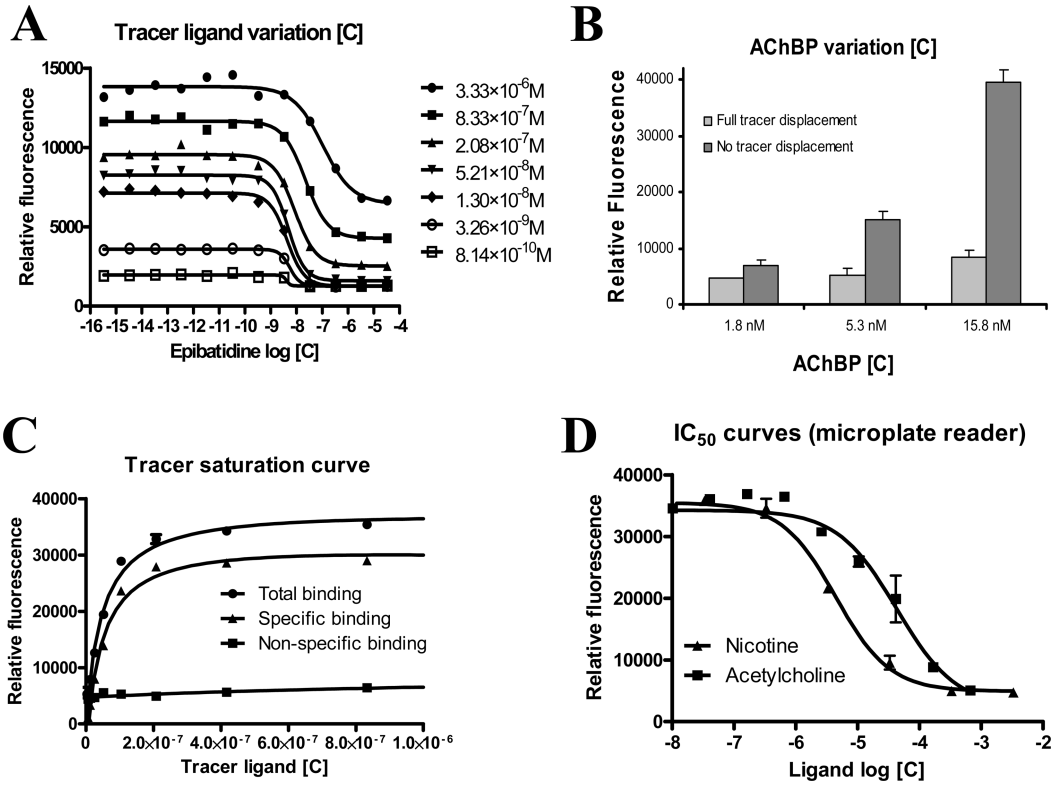

Figure 1. Optimization results in microplate reader format. (A) Variation of tracer ligand ([AChBP] = 2.65 nM). (B) Variation of AChBP ([tracer ligand] = 5.21×10^{-8} M). (C) Tracer saturation curve ([AChBP] = 15.76 nM; nonspecific binding was measured in presence of 10^{-5} M epibatidine). (D) IC_{50} curves of two ligands. [AChBP] = 15.76 nM; [tracer ligand] = 5.21×10^{-8} M.

Analysis of the corresponding IC_{50} values gave 6.98 ± 0.16, 7.65 ± 0.06, 8.07 ± 0.08, 8.32 ± 0.05, 8.37 ± 0.05, 8.26 ± 0.05, and ~8.39, respectively.

In the next step, the effect of the AChBP concentration was studied. These results are depicted in Figure 1B, where no displacement and full displacement are shown. Decreasing the AChBP concentration 3 and 9 times, respectively, also gave approximately the same changes in the assay window. The highest AChBP concentration was used further in order to get a good assay window in the microplate reader format for straightforward evaluation of the assay prior to transfer to the online bioaffinity analysis system (where only 0.158 nM AChBP was used in the assay).

Then, a B_{max} (tracer saturation) curve was constructed as shown in Figure 1C. A concentration of 10^{-5} M epibatidine was used for analysis of nonspecific binding. The three curves in Figure 1C represent the nonspecific binding curve, the total binding curve, and the resulting B_{max} curve. The use of the high concentration of AChBP (15.76 nM) prevented determination of the K_d through the fluorescence enhancement based assay (the apparent K_d found, 47 ± 13 nM, was approximately half of the AChBP binding sites concentration, indicating a titration instead of real binding kinetics). The K_d of DAHBA was therefore determined indirectly with the radioligand binding assay, resulting in a pK_i of 7.59 ± 0.01.

Next, attention was paid to additives and organic modifiers that can either positively influence the assay in general (BSA, ELISA blocking buffer, and Tween 20) or are necessarily introduced in the online bioaffinity analysis format (MeOH, ACN, and DMSO). ELISA blocking reagent and BSA did not influence the assay performance up to 5 mg/mL. MeOH, ACN, DMSO, and Tween 20 decreased assay window to lower than 50% at concentrations of 12%, 13%, 4%, and 5 mg/mL, respectively. It was shown that the optimized assay was stable in a microplate for at least 5 days. The Z'-factor was 0.80 at day one and 0.85 after storage at 4 °C for 5 days. The use of 384-well microplates was also demonstrated and showed the feasibility of this microplate format (Z'-factor of 0.83; data not shown).

Validation of the assay was done with the ligands nicotine and acetylcholine. IC_{50} curves obtained are shown in Figure 1D. Table 2 shows the resulting pK_is for the ligands (calculated from the IC_{50} values by using the Cheng−Prusoff equation.[16] For the ligands measured, small assay discrepancies between

the fluorescence enhancement microplate reader assay and the radioligand binding assay were observed.

Evaluation of the Online Bioaffinity Analysis System. The optimal assay conditions found in microplate reader format were then used in the online bioaffinity analysis system, shown in Figure 2. In the system, injected ligands elute directly from the column in flow injection analysis mode or during gradient HPLC. The eluate is split to the MS and to the bioaffinity analysis system. Here, eluting ligands interact with continuously infused AChBP via the superloop operated by pump $P1_a$ in the first reaction coil (4). In the second reaction coil (6), tracer ligand is continuously infused (via the superloop operated by pump $P2_a$) and interacts with the remaining free binding sites of AChBP. The resulting fluorescence enhancement is monitored by a fluorescence detector. MeOH (70%) with 0.05% formic acid was used through the HPLC column in order to allow direct elution of injected ligands at t_0 (flow injection mode). This setup was preferred instead of a real flow injection analysis setup[17] as injection peaks are minimized. All measurements in this setup were conducted in triplicate. The maximum signal-to-noise ratio obtained was

Table 2. pK_i Values Calculated through the Cheng−Prusoff Equation from Measured IC_{50} Curves[a]

compd	FE plate reader (pK_i)	online (pK_i)	RBA (pK_i)
acetylcholine	4.93 ± 0.16	4.97 ± 0.12	*5.09 ± 0.03*
nicotine	5.91 ± 0.09	5.93 ± 0.02	*6.40 ± 0.01*

[a] Results from three assay formats are compared to evaluate and validate the on-line bioanalysis system. FE, fluorescence enhancement; RBA, radioligand binding assay.

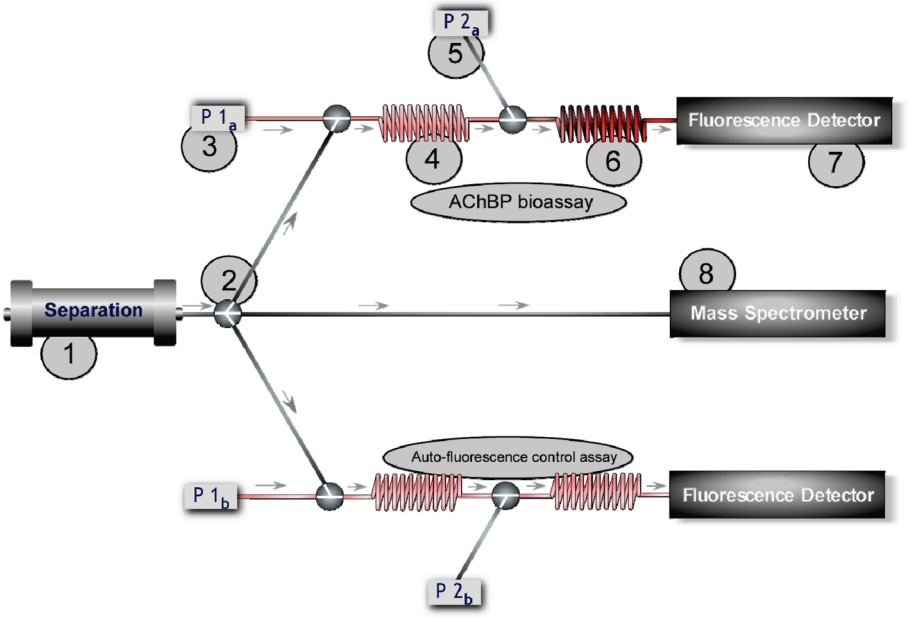

Figure 2. General schematic setup of the online bioaffinity analysis system. Separation (1) with split (2) to the online assay, the online autofluorescence control assay and the MS (8). Online addition of AChBP and tracer ligand (3 and 5). Reaction coils (4 and 6). Fluorescence detection (7). P_{1a} = HPLC pump operating AChBP superloop; P_{1b} is HPLC pump operating a superloop with only buffer. P_{2a} and P_{2b} = HPLC pumps operating superloops with tracer ligand.

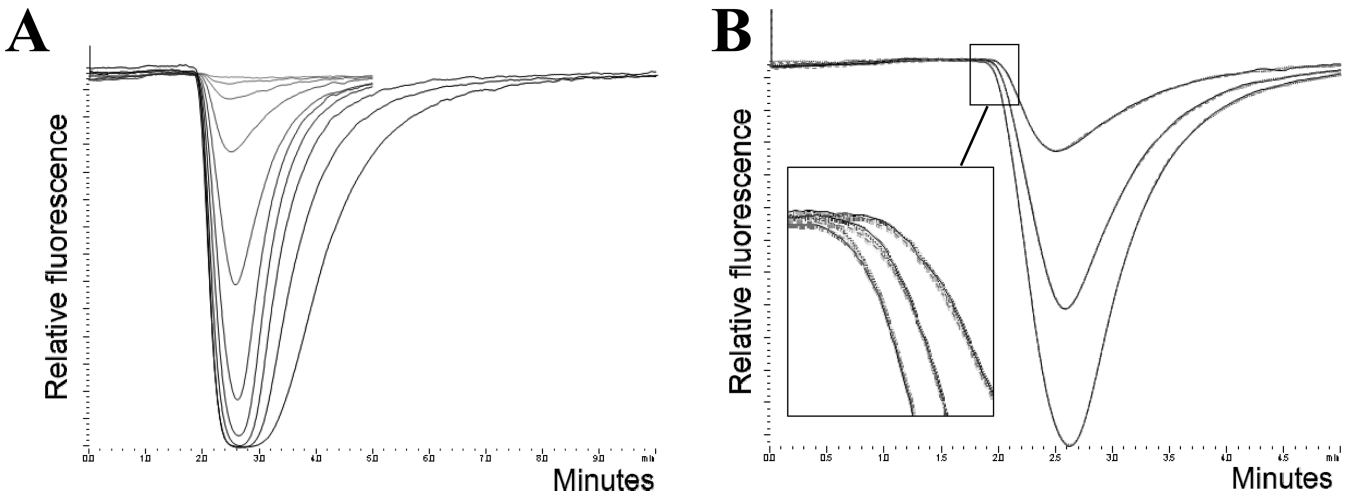

Figure 3. Post column online bioaffinity analysis, minutes vs relative fluorescence. (A) Typical displacement peaks (overlays) from epibatidine injected at different concentrations (highest [C] = 5.1×10^{-6} M; then 1/3 serially diluted). (B) Overlays of triplicate injections from three different concentrations of epibatidine injected (6.3×10^{-8} M, 2.1×10^{-8} M, and 7.0×10^{-9} M).

214 and resulted from injecting epibatidine at a concentration of 10^{-4} M with an AChBP concentration of ~0.158 nM in the online bioaffinity analysis system. Peaks obtained with the system from all concentrations of epibatidine injected are shown in Figure 3A. Injecting different concentrations of epibatidine showed negative peaks of which the peak heights represented the percentages of displacement in the assay. At full displacement, injecting even higher concentrations of epibatidine evidently did not give higher signals but only broader signals due to tailing effects. Figure 3B shows the peaks of three different concentrations of epibatidine injected in triplicate. The figure shows that the triplicate injections for every concentration injected can be perfectly overlaid which demonstrates the reproducibility of the system. The reproducibility was further studied and described analytically and pharmacologically in the next sections.

Pharmacological Validation. As injected compounds are diluted in online bioaffinity analysis systems during the HPLC separation and the online assay, a dilution factor to determine the actual assay concentrations is required. The procedure for determining the dilution factor is described in the Experimental Section. It was found that, upon injection, compounds were diluted 19.7 ± 0.5 times in the online bioaffinity analysis system.

IC_{50} curves were measured for several reference ligands and shown in Figure 4. As ligands are diluted in the online bioaffinity analysis system, it was not possible to measure a complete IC_{50} curve for the low affinity ligands due to solubility problems. For comparison reasons, the IC_{50} values were used to calculate pK_i values (Table 2). The calculated pK_i values correspond well with the results obtained from the fluorescence enhancement based microplate reader assay and the RBA.

Intraday Repeatability. Intraday repeatability was demonstrated by measuring three sequential IC_{50} curves for nicotine during a measuring day (24 h; see Supporting Information Figure S-1A). The online assay did not show a significant decrease in the assay window over time, thus allowing repeatable results over a measuring day. This was reflected by the calculated IC_{50} values, which are depicted in Table 3.

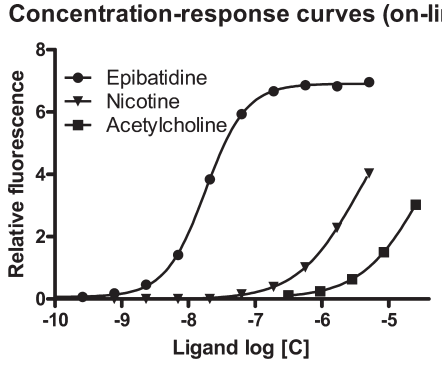

Figure 4. Concentration−response curves of ligands obtained with the online bioaffinity analysis system in flow injection mode.

Furthermore, Z'-factors were determined with data obtained from injecting nicotine at two different concentrations for multiple times (see Supporting Information Figure S-1B). For the higher and lower concentrations of nicotine, Z'-factors of 0.95 and 0.94 were obtained, respectively, indicating an excellent assay performance.[18]

Interday Reproducibility. For interday reproducibility, an IC_{50} curve of nicotine was measured every day for three measuring days with all reagents freshly prepared every day. Here, significant differences in assay window were seen (See Supporting Information Figure S-1C), which were mainly caused by the freeze−thawing process of AChBP causing nonreproducible inactivation. Therefore, the assay window was normalized every day with nicotine injected at a concentration, giving approximately 100% displacement. Subsequently, all other data points during that measuring day were recalculated with the same factor. Supporting Information Figure S-1D gives the normalized IC_{50} curves. Calculation of the IC_{50} values from three measuring days is shown in Table 3, clearly showing very reproducible results.

Ruggedness. As an important factor influencing the online bioaffinity analysis system is the stability of AChBP, ruggedness experiments were focused on this parameter. For this, a batch of AChBP was thawed and used for the first measuring day. Some of the thawed AChBP was kept at 4 °C overnight and used during the second measuring day in a 10 times lower concentration. The rest of the thawed AChBP was frozen again and thawed at the last measuring day of the ruggedness experiments. For every experiment, an IC_{50} curve was measured and normalized the same way as done with the interday experiments. Supporting Information Figure S-1E and S-1F show the original and normalized IC_{50} curves, respectively. It was shown (see Supporting Information Figure S-1F) that widely differing active AChBP concentrations still result in reproducible end results after normalization. This was also supported by the calculated IC_{50} values as seen in Table 3.

Analytical Validation. Sigmodial-Concentration Response Analysis. The online bioaffinity analysis system was inspected by curve fitting of the normalized sigmoidal concentration−response curves obtained during the interday, intraday, and ruggedness experiments. Curve fitting by Graphpad Prism gave curves perfectly crossing all data points measured for every curve analyzed. The quality of fit was determined as the coefficient of determination (r^2) and was found to be higher than 0.979 in all cases (Table 3).

Sensitivity. It should be mentioned that two kinds of assay sensitivity can be distinguished, namely pharmacological and analytical sensitivity. For too high AChBP concentrations, the pharmacological sensitivity decreases for high affinity ligands as displacement binding becomes a titration thus lowering the IC_{50} values found. Second, higher tracer ligand concentrations also decrease the pharmacological sensitivity as more ligand is needed for displacement of the tracer ligand. Lower concentrations of AChBP, therefore, will give a pharmacologically more sensitive assay format in terms of IC_{50} values found. However, for lower AChBP

Table 3. Pharmacological Validation[a]

parameter	1 (IC_{50})	r^2	2 (IC_{50})	r^2	3 (IC_{50})	r^2
intraday	5.39 ± 0.03	0.9983	5.31 ± 0.01	0.9999	5.31 ± 0.01	0.9999
interday	5.48 ± 0.02	0.9990	5.52 ± 0.03	0.9973	5.46 ± 0.07	0.9791
ruggedness	5.62 ± 0.01	0.9999	5.55 ± 0.02	0.9990	5.38 ± 0.03	0.9983

[a] The IC_{50} value of nicotine was determined three times to inspect the intraday repeatability, interday reproducibility, and the ruggedness. The r^2 represents goodness of the curve fitting. The table correlates with Figure S-1 and Table S-2 (Supporting Information).

Table 4. Estimated pK_i Values Analyzed with the Online Bioanalysis System after One Concentration ($n = 3$) Injected[a]

	pK_i from RBA	pK_i at Log [C] = −5.30 injected	pK_i at Log [C] = −5.77 injected	pK_i at Log [C] = −6.25 injected	pK_i at Log [C] = −6.73 injected
5	*6.09 ± 0.06*	5.77 ± 0.00	5.81 ± 0.00	5.84 ± 0.01	5.90 ± 0.02
6	*7.13 ± 0.05*	6.81 ± 0.02	6.76 ± 0.01	6.75 ± 0.01	6.74 ± 0.00
8	*6.29 ± 0.03*	5.97 ± 0.01	5.98 ± 0.01	6.00 ± 0.01	6.02 ± 0.01
9	*8.55 ± 0.02*	7.52 ± 0.03*[b]	8.07 ± 0.02	8.27 ± 0.06	8.23 ± 0.01
10	*7.09 ± 0.03*	6.70 ± 0.01	6.68 ± 0.01	6.69 ± 0.01	6.70 ± 0.00
11	*6.87 ± 0.03*	6.55 ± 0.02	6.54 ± 0.00	6.60 ± 0.00	6.62 ± 0.00
12	*7.00 ± 0.05*	6.80 ± 0.02	6.89 ± 0.02	nd	nd
13	*8.71 ± 0.03*	7.85 ± 0.04*[b]	8.41 ± 0.20	nd	nd
14	*8.46 ± 0.02*	7.46 ± 0.05*[b]	8.08 ± 0.07	8.06 ± 0.02	7.94 ± 0.02
15	*7.38 ± 0.03*	6.77 ± 0.02	6.89 ± 0.00	6.93 ± 0.02	6.95 ± 0.01

[a] The pK_i of every compound was estimated independently after injection at four different concentrations (Log [C] injected of −5.30, −5.77, −6.25, and −6.73). nd, not determined; RBA, radioligand binding assay. [b] *, injected in a too high concentration for good pK_i estimation.

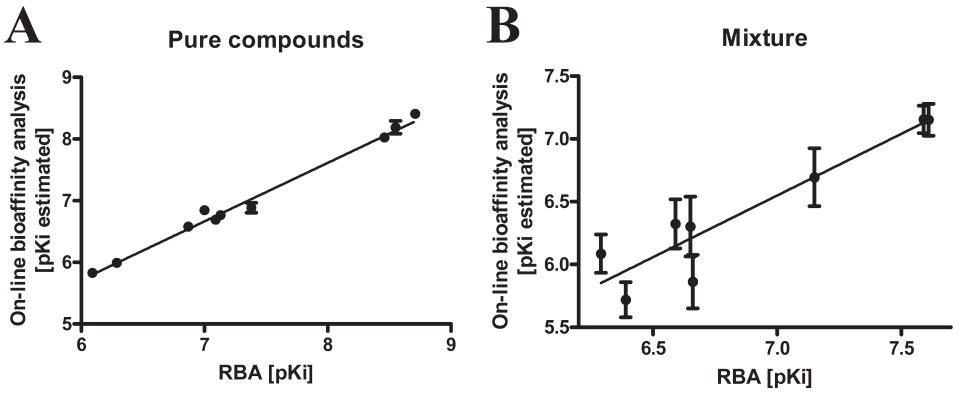

Figure 5. Correlation of estimated affinities from the online bioanalysis system and the RBA. For the online bioanalysis system, the average estimated pK_i of each ligand was calculated with the estimated pK_i values per ligand injected at four different concentrations. (A) Nine individual compounds were analyzed separately at four different concentrations ($r^2 = 0.986$). (B) A mixture of compounds was analyzed at four different concentrations ($r^2 = 0.813$). For the RBA, pK_i values were determined by constructing complete IC_{50} curves ($n = 3$).

and/or tracer ligand concentrations, assay windows will decrease and thus the associated analytical sensitivity. Here, the analytical sensitivity is determined as the limit of detection (LOD), which is the ligand concentration that gives a signal of at least three times the noise. The decrease in analytical sensitivity is nicely observed with the ruggedness experiments for the IC_{50} curve measured at a 10 times lower AChBP concentration. All LODs for nicotine during the validation experiments are depicted in Supporting Information Table S-2 as the lowest depicted concentration for every IC_{50} curve.

Intraday Repeatability, Interday Reproducibility, and Ruggedness. Supporting Information Table S-2 shows the displacement percentages for all concentrations of nicotine tested ($n = 3$) during intraday, interday, and ruggedness experiments. The ruggedness data demonstrated that alterations in the most crucial factor determining assay performance, the AChBP concentration, and/or handling, did not influence the final data markedly. The data shows only large RSDs near the detection limits. Other parameters influencing the assay were evaluated in microplate reader format (e.g., stability toward organic modifiers) and subsequently used in the online bioaffinity analysis system in such a way as to minimize variations in the online bioaffinity analysis readout.

Application of the Online Bioaffinity Analysis System for Single Concentration Based Affinity Ranking. As proof-of-principle demonstration, 10 pure compounds (nonfluorescent anabaseine 5, benzylidene anabaseines 6 and 8−15) as well as a mixture of nine compounds were analyzed with the online bioaffinity analysis system. This was done in an effort to estimate affinities of the ligands by injection of one concentration. For screening purposes, a reliable and reproducible ranking of hits after single concentration injections would be highly valuable.

Pure Compounds. This section demonstrates the affinity estimation of 10 ligands after injection in the online bioaffinity analysis system in one known concentration. Each ligand was subsequently injected in three different concentrations (5, 25, and 125 times diluted), which should result in the estimation of a similar pK_i for every independent ligand. For this, ligand concentrations in the online assay were calculated with use of the dilution factor (see Experimental Section). Then IC_{50} values were calculated from the percentage of displacement measured at the concentration in the assay with the formula used for construction of sigmoidal concentration−response curves ($\%\text{displacement} = 100\%/(1 + 10^{\log\ IC_{50} - \log\ [\text{ligand}]})$). For these affinity estimations, the Hill slope was assumed to be 1. From there, estimated pK_i values were calculated (Table 4). The correlation of these estimated pK_i values with pK_i values from the RBA are represented in Figure 5A, from which an excellent correlation ($r^2 = 0.986$) was found. Any pK_i estimations from very high or very low displacement percentages, however, are less accurate as they represent the shallow curved areas of the sigmoidal concentration−response curves. This was indeed seen for the three ligands with the highest affinity at the highest concentration injected (Table 4; indicated with an asterisk and omitted from the correlation). By a subsequent injection at a lower concentration, as can be deduced from the results, a more accurate result can be obtained.

Mixture of Compounds. For proof-of-concept, a small focused library was constructed from our running drug discovery

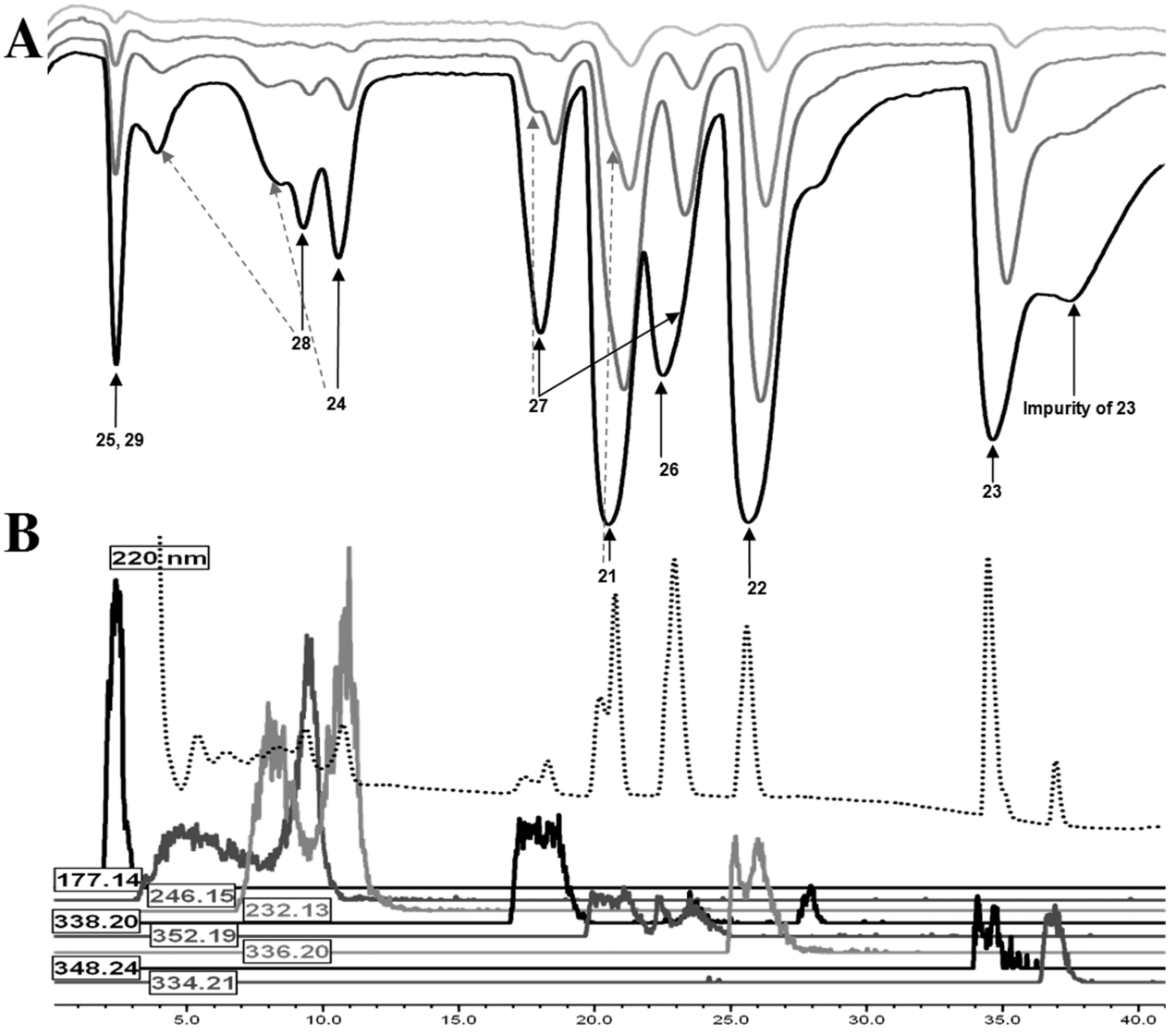

Figure 6. Mixture analysis with the online bioaffinity analysis system. (A) Four bioaffinity chromatograms of a test mixture injected in different concentrations (10^{-4} M of every compound in the mixture for the lowest bioaffinity chromatogram, then 1/5 serially diluted). The compounds were identified with parallel MS and UV detection and correlated with their bioaffinity. All compounds identified are depicted in the figure, where the dashed arrows indicate the same compound in a splitted peak. (B) UV trace (220 nm extracted from DAD) and MS traces of the parent ions from all compounds in the mixture (at 10^{-4} M injected).

programs (nine compounds, **21**−**29**, see Supporting Information Table S-4). Mixture analysis was performed in the same way as discussed for the pure compound library (see previous section) with the difference that the analyses were performed with gradient HPLC runs. In Figure 6A, the bioaffinity traces of a mixture injected in four concentrations are superimposed with the highest concentration represented as the lowest trace. The bioaffinity peaks were assigned to the compounds in the mixture with help of the MS trace, which is shown for the highest concentration of mixture injected in Figure 6B. High resolution IT-TOF MS-MS spectra provided accurate MS-MS data for further structure elucidation. Additionally, Figure 6B shows the UV absorbance at 220 nm extracted from diode array detection (200−300 nm). The strength of the system was highlighted by the identification of an impurity in the mixture (t_r = 37.0 min.), which was determined to be a desmethyl-analogue (m/z 334.21) of **23** (m/z 348.23). Furthermore, the system showed that lobeline (**27**) was present as two isomers, which was confirmed by an independent LC-MS analysis of lobeline (data not shown). Epimerization of lobeline has been described in literature, both in (polar) organic solvents and in buffer solutions.[19,20] Table 5 shows the estimated pK_i values for the individual compounds in the mixture at every mixture concentration injected. As done for the analyses of pure compounds, the estimated pK_i values were correlated with pK_i values from the RBA and presented in Figure 5B, from which a reasonable correlation (r^2 = 0.813) was found.

One critical note is the peak splitting observed, of which the severity decreased upon increasing retention time (Figure 6; indicated per compound by the dashed arrows). As a high injection volume (10 μL) was used to introduce sufficient amounts of compounds in the online bioaffinity assay and the test mixtures were dissolved in MeOH−H_2O (1:1) to prevent precipitation, this was caused by breakthrough of especially the more polar compounds. This thus resulted in division of the compounds over two peaks, which is not a major issue as the bioaffinity trace can be correlated with individual extracted ion chromatograms of the ligands. The actual concentrations of compound in the bioaffinity signals that are analyzed are only slightly lower for most compounds. Only for the early eluting **24** and **28**, severe peak splitting gave

Table 5. Estimated pK_i Values of Compounds in a Mixture Analyzed with the Online Bioanalysis System in Gradient HPLC Mode after One Concentration of Mixture Injected (n = 1 for [Mix C_1]; n = 2 for [Mix $C_{2,3,4}$])[a]

mixture contains	pK_i from RBA	pK_i from HPLC [mix C_1]	pK_i from HPLC [mix C_2]	pK_i from HPLC [mix C_3]	pK_i from HPLC [mix C_4]
21	*7.61 ± 0.12*	7.32	7.14 ± 0.15	7.01 ± 0.06	7.14 ± 0.15
22	*7.59 ± 0.05*	7.30	7.07 ± 0.02	7.07 ± 0.05	7.18 ± 0.14
23	*7.15 ± 0.02*	6.44	6.60 ± 0.04	6.76 ± 0.08	6.98 ± 0.24
24	*6.66 ± 0.07*	5.67	5.83 ± 0.11	6.09 ± 0.19	nd
25	*6.65 ± 0.09*	6.08	6.17 ± 0.05	6.34 ± 0.20	6.62 ± 0.43
26	*6.59 ± 0.03*	6.12	6.34 ± 0.05	6.51 ± 0.13	nd
27 (lobeline)	*6.29 ± 0.01*	5.97	6.03 ± 0.08	6.26 ± 0.19	nd
isomer of lobeline	*nd*	coeluting with **26**	coeluting with **26**	coeluting with **26**	coeluting with **26**
28	*6.39 ± 0.16*	5.58	5.72 ± 0.12	5.86	nd
29	*5.42 ± 0.07*	coeluting with **25**	coeluting with **25**	coeluting with **25**	coeluting with **25**

[a] The pK_i of every compound in the mixture was estimated independently after mixture injection at four different concentrations (see Figure 6). nd, not determined; RBA, radioligand binding assay.

significantly lower concentrations of compound in the bioaffinity signals analyzed and consequently lower pK_i values estimated (see Figure 5B and Table 5). However, this could be anticipated for, which would result in a better correlation in Figure 5B.

Conclusion

This work describes the development of an online bioaffinity analysis system for the acetylcholine binding protein (AChBP). For this, DAHBA, which showed fluorescence enhancement upon binding to AChBP, was first developed. The system underwent a thorough analytical as well as pharmacological validation, revealing a very robust and suitable system delivering data comparable with a traditional radioligand binding assay. The key strength of the system was the capability of estimating and thus ranking affinities of pure compounds at single concentration injections. Furthermore, the system was also capable of estimating affinities of compounds in a focused mixture in combination with their identification after a single gradient HPLC-MS analysis. Thus, we believe that the major surplus value of our methodology is the ability to rapidly and conveniently screen compound libraries and even mixtures of compounds for AChBP affinity. After ranking of the hits with the online bioaffinity analysis system, validation of interesting compounds by measuring complete IC_{50} curves should be performed by injections of multiple concentrations, for further, e.g. SAR, studies. We are currently investigating the screening of a fragment library on AChBP using this methodology.

Experimental Section

General Remarks. The ELISA blocking reagent (BR) was obtained from Hoffmann-La Roche (Mannheim, Germany) and the bovine serum albumin (BSA) came from Gibco BRL (Breda, NL). For the AChBP assays (in microplate reader and in online format), a TRIS/PBS buffer was used with the following composition: 1 mM KH_2PO_4, 3 mM Na_2HPO_4, 0.16 mM NaCl, and 20 mM Trizma-base at pH 7.5 with 400 mg/L ELISA BR.

General Synthetic. The compounds for mixture analyses were synthesized in-house. Chemicals and reagents were obtained from commercial suppliers and were used without further purification. Dry THF was obtained by distillation from CaH_2. Flash column chromatography was typically carried out on a Biotage flash chromatography system, using prepacked Biotage Si 12+M columns, with the UV detector operating at 254 nm. All ^{1}H and ^{13}C NMR spectra were measured on a Brüker 250 or Brüker 400. Analytical HPLC-MS analyses for organic compounds were conducted using two different systems. For **6**−**17**, a Shimadzu LC-20AD liquid chromatograph pump system with a Shimadzu SPD-M20A diode array detector was used, with the MS detection performed with a Shimadzu LCMS-2010 liquid chromatograph mass spectrometer. Conditions: an Xbridge (C18) 5 μm column (4.6 mm × 100 mm) with solvent A (90% MeCN−10% buffer) and solvent B (90% water−10% buffer), flow rate of 1.0 mL/min, start 5% A, linear gradient to 90% A in 8 min, then linear gradient to 5% A in 0.5 min, then 6.5 min at 5% A, total run time of 15 min. For **21**−**29**, a Shimadzu LC-8A preparative liquid chromatograph pump system with a Shimadzu SPD-10AV UV−vis detector with the MS detection performed with a Shimadzu LCMS-2010 liquid chromatograph mass spectrometer. Conditions: an Xbridge (C18) 5 μm column (4.6 mm × 100 mm) with solvent A (90% MeCN−10% buffer) and solvent B (90% water−10% buffer), flow rate of 2.0 mL/min, start 5% A, linear gradient to 90% A in 10 min, then 10 min at 90% A, then 10 min at 5% A, total run time of 30 min. The buffer was a 0.4% (w/v) NH_4HCO_3 solution in water, adjusted to pH 8.0 with NH_4OH. Compound purities were calculated as the percentage peak area of the analyzed compound by UV detection at 254 nm. The compounds were ≥95% pure, unless stated otherwise. A list of all purities is given in the Supporting Information, Table S-3 and S-4.

Synthetic Methods. 5-Chloro-1-(pyridin-3-yl)pentan-1-one (3). In a three-neck flask under N_2, δ-valerolactone **2** (5.0 g, 33 mmol) was dissolved in 200 mL dry THF. This colorless solution was cooled on ice. NaH (60% in mineral oil, 2.0 g, 50 mmol) was added. The gray suspension was stirred at 0 °C for 30 min and at room temperature for another 30 min. The mixture was cooled to 0 °C. To this, a solution of ethylnicotinate **1** (3.0 mL, 22 mmol) in 10 mL dry THF was added dropwise. The reaction mixture was allowed to warm to room temperature overnight while stirring. The solvent was removed under reduced pressure. The resulting solid was suspended in diethylether (200 mL) and collected by vacuum filtration. This solid was mixed with 30 g of crushed ice and concentrated HCl (100 mL) was added. The resulting solution was refluxed during 1 h, cooled to room temperature and poured on 100 g ice. The mixture was basified to pH = 8 and extracted with EtOAc (2 × 150 mL). The organic layers were combined, dried with Na_2SO_4, filtered, and concentrated. The dark-yellow oil was purified with flash column chromatography (eluent: 30% EtOAc/cyclohexane). The product was obtained as a yellow oil (1.47 g, 7.44 mmol, 34%). ^{1}H NMR (250 MHz, $CDCl_3$) δ (ppm) 9.16 (d, J = 1.60 Hz, 1H), 8.77 (dd, J = 4.82, 1.66 Hz, 1H), 8.26−8.17 (m, 1H), 7.42 (ddd, J = 7.98, 4.83, 0.84 Hz, 1H), 3.58 (t, J = 6.18 Hz, 2H), 3.03 (t, J = 6.82 Hz, 2H), 1.99−1.80 (m, 4H).

2-(5-Oxo-5-(pyridin-3-yl)pentyl)isoindoline-1,3-dione (4). Chloride **3** (0.5 g, 2.5 mmol) was dissolved in *N*-methylpyrrolidinone (8 mL). Phthalimide potassium salt (0.47 g, 2.5 mmol) and K_2CO_3 (0.38 g, 2.8 mmol) were added. The dark-yellow suspension was warmed to 90 °C and stirred at this temperature for 4 h.

The reaction mixture was diluted with water (100 mL). This aqueous solution was extracted with DCM (2 × 50 mL). The organic layers were combined, washed thoroughly with water (6 × 50 mL), dried with Na_2SO_4, filtered, and concentrated. A dark-brown oil was obtained (450 mg, 1.46 mmol, 58%). ^{1}H NMR (250 MHz, $CDCl_3$) δ (ppm) 9.16 (d, J = 1.60 Hz, 1H), 8.77 (dd, J = 4.82, 1.66 Hz, 1H), 8.23−8.17 (m, 1H), 7.82 (m, 2H), 7.70 (m, 2H), 7.39 (ddd, J = 7.98, 4.83, 0.84 Hz, 1H), 3.73 (t, J = 6.18 Hz, 2H), 3.04 (t, J = 6.82 Hz, 2H), 1.82−1.75 (m, 4H).

5-Amino-1-(pyridin-3-yl)pentan-1-one·2HBr (5). Phthalimide **4** (450 mg, 1.5 mmol) was mixed with concentrated aq HBr (48%, 7 mL), and the mixture was refluxed overnight. The next day, the reaction mixture was concentrated and recrystallized from hot isopropyl alcohol. The product was obtained as a brown solid (245 mg, 0.72 mmol, 36%). ^{1}H NMR (250 MHz, DMSO) δ (ppm) 9.24 (s, 1H), 8.91 (dd, J = 5.00, 1.51 Hz, 1H), 8.60−8.47 (m, 1H), 7.88−7.56 (m, 4H), 3.16 (d, J = 6.71 Hz, 2H), 2.83 (s, 2H), 1.75−1.56 (m, 4H). ^{13}C NMR (126 MHz, DMSO) δ 198.19, 149.46, 146.03, 140.59, 133.67, 126.23, 39.01, 38.27, 26.78, 20.42.

General Method for Benzylidene Anabaseines. A general procedure reported by Sultana et al. was followed.[21] Amine salt **5** (93 mg, 0.29 mmol) was dissolved in methanol (2 mL). Sodium acetate (33 mg, 0.4 mmol), acetic acid (72 μL, 1.2 mmol), and a substituted benzaldehyde (0.59 mmol) were added to this solution. The dark-yellow solution was refluxed overnight. The reaction mixture was concentrated and dissolved in 1 M aq HCl solution (25 mL). This acidified solution was washed twice with dichloromethane (25 mL). The water layer was basified with Na_2CO_3 and extracted with dichloromethane (3 × 25 mL). The organic layers were combined, dried with Na_2SO_4, filtered, and concentrated. For a few compounds, still present aldehyde was removed by making an HCl salt of the imine and filtering it from ether. If necessary, the compounds were purified with flash column chromatography (eluent: EtOAc/2%TEA), or by formation of the HCl-salt (2 M HCl solution in Et_2O).

(*E*)-3-(3-(4-Dimethylaminobenzylidene)-3,4,5,6-tetrahydropyridin-2-yl)pyridine (7). Synthesized from 5-amino-1-(pyridin-3-yl)pentan-1-one·2HBr (**5**) and 4-dimethylaminobenzaldehyde by the general method described. Yield: 93 mg (0.32 mmol, 36%) of a brown oil. ^{1}H NMR (250 MHz, $CDCl_3$) δ (ppm) 8.78 (d, J = 1.69 Hz, 1H), 8.74−8.64 (m, 1H), 7.89 (dt, J = 7.70, 1.87 Hz, 1H), 7.38 (dd, J = 7.79, 4.83 Hz, 1H), 7.30 (dd, J = 6.80, 1.83 Hz, 3H), 6.72 (d, J = 8.93 Hz, 2H), 6.63 (s, 1H), 3.88 (t, J = 5.53 Hz, 2H), 3.04 (s, 6H), 2.93 (td, J = 6.80, 1.87 Hz, 2H), 1.96−1.82 (m, 2H). ^{13}C NMR (63 MHz, $CDCl_3$) δ 167.97, 150.29, 149.96, 149.68, 137.42, 136.48, 131.56, 127.56, 123.61, 123.02, 111.74, 49.73, 40.19, 26.23, 22.26.

(*E*)-1-methyl-5-((2-(pyridin-3-yl)-5,6-dihydropyridin-3(4H)-ylidene)methyl)indoline (16). Synthesized from 5-amino-1-(pyridin-3-yl)pentan-1-one·2HBr (**5**) and 1-methylindoline-5-carbaldehyde (**20**) by the general method described. Yield: 63 mg (0.21 mmol, 24%) of a red oil. ^{1}H NMR (250 MHz, $CDCl_3$) δ (ppm) 8.77 (dd, J = 2.18, 0.82 Hz, 1H), 8.65 (dd, J = 4.86, 1.71 Hz, 1H), 7.87−7.79 (m, 1H), 7.35 (ddd, J = 7.82, 4.87, 0.86 Hz, 1H), 7.12 (d, J = 7.35 Hz, 2H), 6.58 (s, 1H), 6.45 (d, J = 8.83 Hz, 1H), 3.86 (dd, J = 9.80, 4.19 Hz, 2H), 3.42 (t, J = 8.31 Hz, 2H), 3.00 (t, J = 8.30 Hz, 2H), 2.90 (ddd, J = 6.76, 4.69, 2.12 Hz, 2H), 2.83 (s, 3H), 1.87 (dt, J = 12.04, 6.21 Hz, 2H). ^{13}C NMR (63 MHz, $CDCl_3$) δ 167.82, 153.43, 149.91, 149.42, 136.98, 136.72, 136.38, 130.58, 130.31, 127.70, 125.94, 125.18, 122.93, 106.14, 55.64, 50.09, 35.35, 28.32, 26.34, 22.37.

(*E*)-3-(3-(4-Diethylamino-2-hydroxybenzylidene)-3,4,5,6-tetrahydropyridin-2-yl)pyridine (17, DAHBA). Synthesized from 5-amino-1-(pyridin-3-yl)pentan-1-one·2HBr (**5**) and 4-diethylamino-2-hydroxybenzaldehyde by the general method described. Yield: 50 mg (0.15 mmol, 51%) of a dark-red oil. ^{1}H NMR (500 MHz, DMSO) δ (ppm) 9.28 (s, 1H), 8.64−8.52 (m, J = 4.89 Hz, 2H), 7.78 (dt, J = 7.80, 1.93 Hz, 1H), 7.41 (dd, J = 7.80, 4.84 Hz, 1H), 7.23 (d, J = 8.85 Hz, 1H), 6.73 (s, 1H), 6.19 (dd, J = 8.84, 2.50 Hz, 1H), 6.12 (d, J = 2.51 Hz, 1H), 3.70 (t, J = 5.48 Hz, 2H), 3.29 (q, J = 7.00 Hz, 4H), 2.73 (t, J = 5.65 Hz, 2H), 1.81−1.63 (m, 2H), 1.08 (t, J = 7.00 Hz, 6H). ^{13}C NMR (126 MHz, DMSO) δ 166.83, 157.44, 149.27, 149.11, 148.85, 136.68, 136.17, 130.66, 130.54, 125.59, 122.93, 110.11, 102.92, 97.55, 49.39, 43.77, 25.87, 22.24, 12.58. HR-MS m/z [M + H] 336.2086, error[ppm] = −4.6. LC-purity: >99% (220 and 254 nm).

1-Methylindoline (19). Indoline **18** (2.8 mL, 25.2 mmol) was added to K_2CO_3 (1.5 g, 10.9 mmol) in 20 mL of DMF. Dimethylcarbonate (6.4 mL, 76 mmol) was added. The yellow mixture was refluxed overnight. It was cooled to room temperature and 50 mL of water was added. The product was extracted with 60 mL of *tert*-butylmethylether. The organic layer was washed with water (3 × 50 mL), dried with Na_2SO_4, filtered, and concentrated. The product was purified with flash column chromatography, eluent: gradient of hexane/ethyl acetate. Yield: 500 mg (3.75 mmol, 15%) of a pale-yellow oil. ^{1}H NMR (250 MHz, $CDCl_3$) δ (ppm) 7.12 (m, 2H), 6.70 (t, J = 7.36 Hz, 1H), 6.58−6.49 (d, J = 8.18 Hz, 1H), 3.35 (t, J = 8.08 Hz, 2H), 3.00 (t, J = 8.16 Hz, 2H), 2.82 (s, 3H).

1-Methylindoline-5-carbaldehyde (20). DMF (0.70 mL, 13.7 mmol) and $POCl_3$ (0.27 mL, 3.0 mmol) were dissolved in 1,2-dichloroethane (2.5 mL). Then 1-methylindoline (**19**) in 1,2-dichloroethane (2.5 mL) was added. The dark-yellow solution was refluxed during 3 h. Saturated $NaHCO_3$ solution (20 mL) and dichloromethane (20 mL) were added. The layers were separated, and the water layer was extracted with dichloromethane (20 mL). The combined organic layers were dried with Na_2SO_4, filtered, and concentrated. Yield: 244 mg. ^{1}H NMR analysis revealed that the crude product contained 60% product and 40% doubly formylated product as byproduct. The product was used without further purification. ^{1}H NMR (250 MHz, $CDCl_3$) δ (ppm) 9.72 (s, 1H), 7.60 (s, 2H), 6.44 (d, J = 8.26 Hz, 1H), 3.60 (t, J = 8.46 Hz, 2H), 3.06 (dd, J = 18.05, 9.48 Hz, 2H), 2.93 (s, 3H).

Protein Production and Purification. Ls-AChBP (from snail species *Lymnaea stagnalis*) was expressed from baculovirus using the pFastbac I vector in Sf9 insect cells and purified from medium as described by Celie et al.[1]

UV and Fluorescence Enhancement Properties of Benzylidene Anabaseines. Dilution series, consisting of five concentrations between 5×10^{-5} M and 5×10^{-6} M, were made from a 1×10^{-2} M solution in DMSO, using the TRIS/PBS buffer described. UV spectra were recorded using a Cary 50 Conc UV/vis spectrometer. The λ_{max} values and ε values were determined. This λ_{max} was used to measure the fluorescence of the compounds at 5×10^{-6} M concentrations using a Perkin-Elmer LS50B fluorescence meter in the absence and presence of ~42 nM Ls-AChBP (625 ng/μL, 5 μL added to 3 mL compound solution in buffer). Fluorescence of Ls-AChBP is neglectable when $\lambda_{excitation}$ > 400 nm. For compounds with lower λ_{max} values, no fluorescence enhancement was found, either because there was no measurable enhancement or due to background fluorescence of the protein.

Fluorescence Enhancement Microplate Reader Assay. A Novostar (with software version 1.20−0) from BMG Labtechnologies (Offenburg, Germany) was used in fluorescence mode for the plate reader assays. The excitation and emission wavelengths were 485 and 520 nm, respectively. Black-bottomed PP-96-well (and PP-384-well) microtiter plates from Greiner Bio-one (Alphen a/d Rijn, NL) were used. For all microplate reader measurements, 30 μL of ligand or different concentrations organic modifier, blocking reagents or detergent, 30 μL of Ls-AChBP, and 30 μL of DAHBA were added subsequently. DAHBA was added 5 min after addition of the AChBP, followed by incubation at room temperature for 10 min before readout. In the manuscript, only the final concentrations are depicted.

Radioligand Binding Assay. A radioligand binding assay (96-well format) was conducted to compare the results obtained with the fluorescence enhancement assay. Ls-AChBP was diluted in PBS-Tris binding buffer (final concentration of 1.4 mM KH_2PO_4, 4.3 mM Na_2HPO_4, 137.0 mM NaCl, 2.7 mM KCl, 20 mM Trizma-base, 4% DMSO, 0.05% Tween 20, pH 7.4) to obtain a quantity of 1.3 ng per well. Ls-AChBP was incubated

with $10^{-4}-10^{-11}$ M of ligands (from stock solutions of 10 mM in DMSO) in the presence of approximately 1.5 nM [^{3}H]epibatidine (K_D = 0.875 nM, Perkin-Elmer Life Science, Inc., USA) and 0.2 mg PVT Copper His-Tag SPA beads (GE healthcare). Final well volume was 100 μL and the incubation time was 60 min followed by 3 h in the absence of light. Thereafter the label−bead complexes were counted in a micro beta counter.

Online Bioaffinity Analysis. A similar setup described by de Vlieger et al. was used.[22] Figure 2 shows a schematic drawing of the system used. A Shimadzu ('s Hertogenbosch, The Netherlands) SIL20 autoinjector introduced the samples into the system (10 μL injections) followed by separation with a Waters (Milford, MA) Xterra C18MS column (2.1 mm × 100 mm, 3.5 μm particles) and guard column. Mobile phase A consisted of H_2O−MeOH−formic acid (98.9%−1%−0.1%) and mobile phase B of MeOH−H_2O−formic acid (98.9%−1%−0.1%). In flow-injection analysis mode for analysis of pure compounds, 30/70% mobile phase A/B was used at a flow rate of 125 μL/min. For gradient elution, the following gradient was used: 0−2 min at 20% mobile phase B followed by a linear increase to 50% mobile phase B in 33 min, then a linear increase to 100% mobile phase B in 2 min followed by 3 min at 100% mobile phase B. Equilibration occurred by performing a linear decrease to 20% mobile phase B in 1 min followed by 4 min at 20% mobile phase B. After the LC column, a split of 125:125:1000 directed the flow to the parallel assays and MS, respectively. The LC-MS system consisted of a Shimadzu LCMS-IT-TOF with a SPD20 M photodiode array detector. The ion-trap time-of-flight (IT-TOF) MS was operated in data dependent acquisition mode switching between full-spectrum MS and MS-MS modes. The electrospray (ESI) source was operated in positive ion mode. The temperature of the heating block and curved desolvation line was set to 200 °C. Interface voltage was set at 4.5 kV, the nebulizing gas flow (nitrogen, 99.999% purity, Praxair, Oevel, Belgium) was 1.5 L/min, and drying gas was applied at a pressure of 65 kPa. Full MS spectra were acquired from m/z 50−700. MS-MS data was obtained automatically with 25 ms accumulation time from m/z 50−700 and a precursor isolation width of 3.0 using argon (99.9995% purity, Praxair) as collision gas. The bioaffinity analysis part employed four Shimadzu LC10ADvp pumps and two Shimadzu RF10-XL fluorescence detectors (λ_{ex} = 485 nm, λ_{em} = 526 nm). One of the online assays was used as autofluorescence control assay in which AChBP was omitted from its superloop (via $P1_b$). This allowed the detection of false positive ligands that display intrinsic fluorescence at the wavelengths used for bioaffinity analysis. For the actual online assay, the AChBP concentration was 0.345 nM in superloop 1 (representing 0.158 nM in the assay). The concentration of tracer ligand DAHBA was 150 nM in superloop 2 (representing 68 nM in the assay). The superloops were operated at a flow rate of 70 μL/min and were kept on ice. The assays were performed in a thermostatted oven at 37 °C. The volumes of the first and second reaction coils (of PEEK material) were 25 and 20 μL, respectively. For analysis of IC_{50} values, 10^{-2} M solutions of ligands or mixtures of ligands in DSMO were diluted in MeOH−H_2O (1:1) to 10^{-4} M solutions. These solutions, or dilutions thereof, were injected into the system and the resulting percentages of displacement were used for IC_{50} value calculations.

Dilution Factor. The dilution factor after injection into the online bioaffinity analysis system was determined by a calibration process. For this, the fluorescent compound resorufin (100 nM in buffer) was pumped into the online bioaffinity analysis system via one superloop, while the other superloop only contained buffer. The resulting increased fluorescent signal was recorded. Then, the resorufin solution was replaced by buffer and the resorufin solution was subsequently injected (10 μL) into the online bioaffinity analysis system. The peak heights of eluting resorufin were compared with the elevated fluorescent signal from which the dilution factor of resorufin in the online bioaffinity analysis system was be determined.

Software. LCMS Solution from Shimadzu was used for analysis of all data obtained with the online bioaffinity analysis system (LC, MS and fluorescence enhancement data). Graphpad Prism 4 was used for curve fitting and determination all biochemical parameters (e.g., IC_{50} values, pK_i values, K_ds and B_{max} values).

Acknowledgment. We thank Shimadzu for their instrumental support. We thank Ewald Edink for providing compounds for the focused compound library. ABS, GdK, and IdE were supported by Top Institute Pharma grant D2-103.

Supporting Information Available: Pharmacological and analytical validation of the on-line system. Purities and HR-MS data for all in-house synthesized compounds. Spectral properties and synthetic routes of some of the compounds used. This material is available free of charge via the Internet at http://pubs.acs.org.

References

(1) Celie, P. H.; Kasheverov, I. E.; Mordvintsev, D. Y.; Hogg, R. C.; van Nierop, P.; van Elk, R.; van Rossum-Fikkert, S. E.; Zhmak, M. N.; Bertrand, D.; Tsetlin, V.; Sixma, T. K.; Smit, A. B. Crystal structure of nicotinic acetylcholine receptor homolog AChBP in complex with an alpha-conotoxin PnIA variant. *Nat. Struct. Mol. Biol.* **2005**, *12*, 582–588.

(2) Dutertre, S.; Ulens, C.; Buttner, R.; Fish, A.; van Elk, R.; Kendel, Y.; Hopping, G.; Alewood, P. F.; Schroeder, C.; Nicke, A.; Smit, A. B.; Sixma, T. K.; Lewis, R. J. AChBP-targeted alpha-conotoxin correlates distinct binding orientations with nAChR subtype selectivity. *EMBO J.* **2007**, *26*, 3858–3867.

(3) Hogg, R. C.; Bertrand, D. Nicotinic acetylcholine receptors as drug targets. *Curr. Drug Targets CNS Neurol. Disord.* **2004**, *3*, 123–130.

(4) Hogg, R. C.; Raggenbass, M.; Bertrand, D. Nicotinic acetylcholine receptors: from structure to brain function. *Rev. Physiol. Biochem. Pharmacol.* **2003**, *147*, 1–46.

(5) Smit, A. B.; Syed, N. I.; Schaap, D.; van Minnen, J.; Klumperman, J.; Kits, K. S.; Lodder, H.; van der Schors, R. C.; van Elk, R.; Sorgedrager, B.; Brejc, K.; Sixma, T. K.; Geraerts, W. P. A glia-derived acetylcholine-binding protein that modulates synaptic transmission. *Nature* **2001**, *411*, 261–268.

(6) Sharma, J.; Besanger, T. R.; Brennan, J. D. Assaying small-molecule-receptor interactions by continuous flow competitive displacement chromatography/mass spectrometry. *Anal. Chem.* **2008**, *80*, 3213–3220.

(7) Jozwiak, K.; Haginaka, J.; Moaddel, R.; Wainer, I. W. Displacement and nonlinear chromatographic techniques in the investigation of interaction of noncompetitive inhibitors with an immobilized alpha3beta4 nicotinic acetylcholine receptor liquid chromatographic stationary phase. *Anal. Chem.* **2002**, *74*, 4618–4624.

(8) Jozwiak, K.; Moaddel, R.; Yamaguchi, R.; Ravichandran, S.; Collins, J. R.; Wainer, I. W. Qualitative assessment of IC_{50} values of inhibitors of the neuronal nicotinic acetylcholine receptor using a single chromatographic experiment and multivariate cluster analysis. *J. Chromatogr., B: Anal. Technol. Biomed. Life Sci.* **2005**, *819*, 169–174.

(9) Brejc, K.; van Dijk, W. J.; Klaassen, R. V.; Schuurmans, M.; van Der Oost, J.; Smit, A. B.; Sixma, T. K. Crystal structure of an ACh-binding protein reveals the ligand-binding domain of nicotinic receptors. *Nature* **2001**, *411*, 269–276.

(10) Gao, F.; Mer, G.; Tonelli, M.; Hansen, S. B.; Burghardt, T. P.; Taylor, P.; Sine, S. M. Solution NMR of acetylcholine binding protein reveals agonist-mediated conformational change of the C-loop. *Mol. Pharmacol.* **2006**, *70*, 1230–1235.

(11) Hansen, S. B.; Radic, Z.; Talley, T. T.; Molles, B. E.; Deerinck, T.; Tsigelny, I.; Taylor, P. Tryptophan fluorescence reveals conformational changes in the acetylcholine binding protein. *J. Biol. Chem.* **2002**, *277*, 41299–41302.

(12) van Elswijk, D. A.; Diefenbach, O.; van der Berg, S.; Irth, H.; Tjaden, U. R.; van der Greef, J. Rapid detection and identification of angiotensin-converting enzyme inhibitors by on-line liquid chromatography-biochemical detection, coupled to electrospray mass spectrometry. *J. Chromatogr., A* **2003**, *1020*, 45–58.

(13) Schenk, T.; Breel, G. J.; Koevoets, P.; van den Berg, S.; Hogenboom, A. C.; Irth, H.; Tjaden, U. R.; van der Greef, J. Screening of natural products extracts for the presence of phosphodiesterase inhibitors using liquid chromatography coupled online to parallel biochemical detection and chemical characterization. *J. Biomol. Screening* **2003**, *8*, 421–429.

(14) Schobel, U.; Frenay, M.; van Elswijk, D. A.; McAndrews, J. M.; Long, K. R.; Olson, L. M.; Bobzin, S. C.; Irth, H. High resolution screening of plant natural product extracts for estrogen receptor alpha and beta binding activity using an online HPLC-MS biochemical detection system. *J. Biomol. Screening* **2001**, *6*, 291–303.
(15) Talley, T. T.; Yalda, S.; Ho, K. Y.; Tor, Y.; Soti, F. S.; Kem, W. R.; Taylor, P. Spectroscopic analysis of benzylidene anabaseine complexes with acetylcholine binding proteins as models for ligand-nicotinic receptor interactions. *Biochemistry* **2006**, *45*, 8894–8902.
(16) Cheng, Y.; Prusoff, W. H. Relationship between the inhibition constant (K1) and the concentration of inhibitor which causes 50% inhibition (I_{50}) of an enzymatic reaction. *Biochem. Pharmacol.* **1973**, *22*, 3099–3108.
(17) Kool, J.; van Liempd, S. M.; Ramautar, R.; Schenk, T.; Meerman, J. H.; Irth, H.; Commandeur, J. N.; Vermeulen, N. P. Development of a novel cytochrome p450 bioaffinity detection system coupled online to gradient reversed-phase high-performance liquid chromatography. *J. Biomol. Screening* **2005**, *10*, 427–436.
(18) Zhang, J. H.; Chung, T. D.; Oldenburg, K. R. A Simple Statistical Parameter for Use in Evaluation and Validation of High Throughput Screening Assays. *J. Biomol. Screening* **1999**, *4*, 67–73.
(19) Compere, D.; Marazano, C.; Das, B. C. Enantioselective access to *Lobelia* alkaloids. *J. Org. Chem.* **1999**, *64*, 4528–4532.
(20) Crooks, P. A.; Dwoskin, L. P. Use of lobeline epimers in the treatment of central nervous system diseases, pathologies, and drug abuse. WO Patent Application 2009/059260, 2009.
(21) Sultana, I.; Ikeda, I.; Ozoe, Y. Structure−activity relationships of benzylidene anabaseines in nicotinic acetylcholine receptors of cockroach nerve cords. *Bioorg. Med. Chem.* **2002**, *10*, 2963–2971.
(22) de Vlieger, J. S.; Kolkman, A. J.; Ampt, K. A.; Commandeur, J. N.; Vermeulen, N. P.; Kool, J.; Wijmenga, S. S.; Niessen, W. M.; Irth, H.; Honing, M. Determination and identification of estrogenic compounds generated with biosynthetic enzymes using hyphenated screening assays, high resolution mass spectrometry and off-line NMR. *J. Chromatogr., B: Anal. Technol. Biomed. Life Sci.* **2010**, *878*, 667–674.